Atmospheric
Chemistry
and Physics

Open Access

EGU

Supplement of

Molecular insight into aqueous-phase photolysis and photooxidation of water-soluble organic matter emitted from biomass burning and coal combustion

Tao Cao et al.

Correspondence to: Jianzhong Song (songjzh@gig.ac.cn)

S1. Sample information

Rice straw (RS) and Yulin coal (YL) were selected as representative biomass and coal fuel materials for the preparation of combustion-derived WSOM samples. RS was collected in Chuzhou, Anhui Province. As shown in Table S1, the carbon (C), hydrogen (H), oxygen (O), nitrogen (N) and ash contents of RS were 38.3%, 5.74%, 43.8%, 1.90% and 10.3%, respectively. Prior to combustion, RS was sorted and cut into smaller sections to enhance the efficiency of the combustion process. YL coal was collected from Yulin, Shanxi Province. The maturity and volatile content of YL coal were determined to be 0.58% and 34.4%, respectively, confirming its classification as high volatile bituminous coal. Additionally, the ash content of YL coal was measured at 4.22% and the C, H, O, N and S contents of YL coal were 77.0%, 6.07%, 11.6%, 1.01% and 0.17%, respectively.

S2. WSOM extraction and measurement

The weighted smoke filters were fragmented into small pieces and subsequently placed into a pre-baked 100 mL glass bottle. Then, 60 mL of ultrapure water was added, and the mixture was subjected to sonication at a constant temperature of 25°C for a duration of 30 min. The supernatant was filtered through a 0.22 μm PTFE membrane, resulting in a solution that serves as the stock solution of water-soluble organic matter (WSOM). The concentration of the WSOM stock solution was quantified using a total organic carbon analyzer (VCPH analyzer, Shimadzu, Kyoto, Japan) in accordance with the non-purgeable organic carbon protocol. After the removal of inorganic carbon, the sample underwent oxidation at a high temperature of

680°C, and the peak area of CO_2 was measured using a non-dispersive infrared detector. The WSOM stock solution was subsequently diluted to approximately 20 mgC/L with ultrapure water, based on the measured concentration. Photolysis experiments will be conducted utilizing this diluted solution.

S3. Optical properties analysis

The absorption coefficient (α_λ, m^{-1}) was calculated to estimate the abundance of typical chromophores within WSOM and it can be calculated as following equation:

$$\alpha_\lambda = 2.303 \times \frac{A_\lambda}{l} \tag{S1}$$

In this equation, the absorbances at 254nm and 365nm were used (A_λ), l represents light path (0.01m). The α_{254} value indicates the content of aromatic structures and double bonds, which was positively correlated with the amounts and properties of aromatic components. The α_{365} value represents the light absorption of WSOM in near ultraviolet and visible ranges, which had been widely used to characterize brown carbon (BrC) in atmospheric environments (Hecobian et al., 2010; Jiang et al., 2021b).

The absorption was normalized by organic carbon mass which defined as mass absorbance efficiency (MAE), the MAE at 365 nm (MAE$_{365}$) is an important optical parameter used to characterize the light absorbing capacity of WSOM. It was obtained using the following equation:

$$MAE_\lambda = \frac{A_\lambda}{c*l} * ln(10) \tag{S2}$$

where A_λ is the absorbance at λ nm, c is the carbon concentration of BrC in solution (mgC

L^{-1}), and l is the absorbing path length (0.01m).

The absorption Ångström exponent (AAE) is a measure of the spectral dependence of the light absorption of WSOM solutions, which was calculated by the following equation:

$$A_\lambda = K\lambda^{-AAE} \tag{S3}$$

where A_λ is the absorbance derived from the spectrophotometer at a given wavelength λ (330–400 nm) and K is a constant.

The PARAFAC was computed using two to nine component models, with non-negativity constraints and a residual analysis; and split half analysis was used to validate the number of fluorescence components. According to the results of the split-half and core consistency analysis, three component models were chosen for further analysis. The identified individual fluorophores were compared with online database OpenFluor (based on the identified fluorophores in nature organic matter and the similarity of results for both excitation and emission wavelength were set at 98%). The relative contribution of individual chromophores was estimated by calculating the maximum fluorescence intensities (F_{max}: maximum fluorescence intensity of identified fluorescence components, relative content % = Fmax/ΣF_{max}).

S4. FT-ICR MS analysis

The samples were ionized in negative-ion mode using an Electrospray Ionization (ESI) source. The ion accumulation time was set to 0.65s and a total of 100 continuous 4M data FT-ICR transients were added to enhance the signal-to-noise ratio and the dynamic range. The

detection mass range was set to m/z 100–800. Mass spectra were calibrated externally with arginine clusters in negative-ion mode using a linear calibration. The final spectrum was internally recalibrated with typical O_5-class species peaks using quadratic calibration in DataAnalysis 4.4 (Bruker Daltonics). A typical mass-resolving power (m/Δm50%, where Δm50% is the magnitude of the mass spectral peak full-width at half-maximum peak height) > 450,000 at m/z 319 with < 0.2 ppm absolute mass error was achieved.

The ultrahigh-resolution FT-ICR mass spectra were processed with custom software. All ions with relative abundances greater than 10 times the standard deviation of the baseline noise were explored. Mathematically possible formulae for these ions were then calculated with a mass tolerance of ± 1 ppm. The formula CcHhOoNnSs was used to indicate the assigned compounds, in which C, H, O, N, S indicate carbon, hydrogen, oxygen, nitrogen, and sulfur, respectively, and c, h, o, n, s represent the number of atoms of the respective elements. The maximum numbers of atoms for the formula calculator were set as follows: 30 ^{12}C, 60 ^{1}H, 20 ^{16}O, 3 ^{14}N, 1 ^{32}S, 1 ^{13}C, 1 ^{18}O, and 1 ^{34}S. The identified formulae containing isotopomers (i.e., ^{13}C, ^{18}O, or ^{34}S) are not discussed. The calculated formulae were further characterized in terms of double-bond equivalents (DBE) and the modified aromaticity index (AImod), based on calculation of the elemental composition CcHhOoNnSs. The DBE value represents the number of rings plus double bonds, which reflects the degree of unsaturation (hydrogen deficiency) in a given compound. The DBE value can be calculated according to Equation (S4):

$$DBE = \frac{2c+2-h+n}{2} \qquad\qquad (S4)$$

All calculated formulae with DBE < 0 and that disobey the nitrogen rule for even- number

electron ions were excluded from the lists. The AImod value of each molecular formula was

estimated based on the equation proposed by Koch and Dittmar:

$$AI_{mod} = \frac{1+c-0.5o-s-0.5h}{c-0.5o-s-n} \qquad (S5)$$

Based on the AI_{mod} values, the molecular formulae can be tentatively classified as aliphatic

($AI_{mod, w} = 0$), non-aromatic compounds ($0 < AI_{mod} < 0.5$), aromatic ($0.5 \leqslant AI_{mod} \leqslant 0.67$)

and condensed aromatic ($0.67 < AI_{mod}$).

The nominal oxidation state of carbon (NOSC) was used as the degree of oxidation of

organic matter, which can be obtained according to the following equation (LaRowe et al.,

2011):

$$NOSC = 4 - \frac{4c+h-3n-2o-2s}{c} \qquad (S6)$$

In the study, the overall properties of the WSOM fractions were assessed with relative

abundance weighting because each molecule was present with different intensity. The relative-

abundance-weighted molecular weight, elemental ratios, DBE, and AI_{mod} were calculated from

the intensity (Int) of each assigned peak (i) based on the following equations:

$MW_w = \Sigma(MW_i*Int_i)/\Sigma Int_i$

$OM/OC_w = \Sigma(OM/OC_i*Int_i)/\Sigma Int_i$

$O/C_w = \Sigma(O/C_i*Int_i)/\Sigma Int_i$

$O/N_w = \Sigma(O/N_i*Inti)/\Sigma Int_i$

$O/S_w = \Sigma(O/S_i*Int_i)/\Sigma Int_i$

$DBE_w = \Sigma(DBE_i*Int_i)/\Sigma Int_i$

$AI_{mod,w} = \Sigma(AI_{mod,i}*Int_i)/\Sigma Int_i$

$$NOSC_{,w}= \Sigma(NOSC\times Int_i)/ \Sigma Int_i$$

where Int_i is the intensity for each individual molecular formula, i.

Although the negative ESI- FT-ICR MS provided detailed information of WSOM, it should be noted that the composition information is incomplete. According to previous studies, different ionization sources are favorable for different compounds. In fact, BrC is a complex of light-absorbing compounds, the solvent-extractable BrC light absorption is not only attributed to polar compounds but also due to the water-insoluble and less polar compounds such as PAHs and their derivatives. Therefore, other ionization techniques such as positive-ion ESI and APPI are complementary to the negative-ion analysis in further studies.

Table S1. Basic information and elemental composition of rice straw and Yulin coal

	Rice straw (RS)	Yulin coal (YL)
C (%)	38.3	77.0
H (%)	5.74	6.07
O (%)	43.8	11.6
N (%)	1.90	1.01
S (%)	-	0.17
Ash (%)	10.3	4.22
Maturity (%)	-	0.58
Volatile (%)	-	34.4
Rank	-	High volatile bituminous coal

Table S2. The intensity-weighted average elemental ratios, DBE_w, DBE/C_w, $AI_{mod,w}$ and $NOSC_w$ of molecular formulas in RS and YL WSOM for fresh, after photolysis and after ·OH photooxidation.

Samples		Composition	MW_w	H/C_w	O/C_w	O/N_w	O/S_w	DBE_w	DBE/C_w	$AI_{mod,w}$	$NOSC_w$
		CHO	236	1.19	0.38			5.98	0.50	0.43	-0.43
		CHON	298	1.17	0.36	4.24		7.88	0.55	0.50	-0.14
	Fresh	CHOS	292	1.28	0.55		6.25	5.31	0.45	0.22	-0.01
		CHONS	327	1.29	0.56	6.50	6.88	6.16	0.48	0.23	0.27
		Total	252	1.19	0.38	1.05	0.19	6.40	0.51	0.44	-0.35
		CHO	267	1.17	0.44			6.63	0.50	0.41	-0.29
		CHON	342	1.15	0.39	5.14		8.89	0.54	0.47	-0.08
RS WSOM	Photolysis	CHOS	310	1.39	0.48		5.73	5.16	0.39	0.21	-0.25
		CHONS	310	1.33	0.59	6.51	6.63	5.51	0.47	0.20	0.30
		Total	288	1.17	0.43	1.38	0.10	7.20	0.51	0.42	-0.23
		CHO	302	1.16	0.60			6.73	0.50	0.35	0.04
		CHON	355	1.15	0.57	7.45		8.55	0.55	0.41	0.28
	·OH Photooxidation	CHOS	389	1.09	0.44		6.16	11.73	0.52	0.37	-0.10
		CHONS	362	1.34	0.68	7.14	7.14	8.53	0.47	0.20	0.50
		Total	319	1.16	0.59	1.88	0.26	7.36	0.52	0.36	0.10

Continued Table S2

Samples		Composition	MW_w	H/C_w	O/C_w	O/N_w	O/S_w	DBE_w	DBE/C_w	$AI_{mod,w}$	$NOSC_w$
YL WSOM	Fresh	CHO	218	0.95	0.39			7.07	0.62	0.60	-0.17
		CHON	227	1.03	0.51	4.39		6.59	0.66	0.66	0.36
		CHOS	255	1.23	0.56		5.34	5.14	0.49	0.28	0.10
		CHONS	361	1.19	0.54	7.32	7.32	7.72	0.52	0.32	0.26
		Total	231	1.03	0.46	1.62	1.07	6.60	0.61	0.56	0.06
	Photolysis	CHO	255	0.98	0.43			7.65	0.60	0.55	-0.13
		CHON	326	1.00	0.42	6.02		9.79	0.62	0.58	0.09
		CHOS	279	1.31	0.52		5.65	5.25	0.44	0.26	-0.07
		CHONS	326	1.22	0.53	6.59	6.59	6.77	0.52	0.32	0.27
		Total	268	1.02	0.43	0.89	0.60	7.70	0.59	0.52	-0.09
	·OH Photooxidation	CHO	293	1.02	0.57			7.54	0.57	0.46	0.12
		CHON	357	1.00	0.54	8.01		9.93	0.61	0.52	0.30
		CHOS	342	1.16	0.51		6.38	8.64	0.50	0.32	0.01
		CHONS	460	0.97	0.39	5.23	5.23	17.95	0.62	0.51	0.16
		Total	303	1.02	0.57	1.10	0.14	7.90	0.58	0.47	0.14

Table S3. Relative abundances (%) of seven categories components within RS and YL WSOM for fresh, after photolysis and after ·OH photooxidation.

Samples		Lipids	Protein	Carbohydrate	Unsaturated	Lignin	Condensed	Tannins
RS WSOM	Fresh	5.69	7.19	0.67	0.36	83.1	1.08	1.91
	Photolysis	2.81	7.18	0.86	0.18	84.6	1.55	2.77
	·OH Photooxidation	0.074	4.94	3.69	0.13	63.3	4.86	23.0
YL WSOM	Fresh	0.52	1.67	0.36	0.31	88.4	2.86	5.86
	Photolysis	0.51	3.11	0.53	0.16	88.7	4.08	2.92
	·OH Photooxidation	0.052	2.32	0.96	0.032	73.9	5.38	17.3

Table S4. The number and percentage of molecules resistant, degraded and produced during photolysis and ·OH photooxidation for RS and YL WSOM.

Samples	Aging processes	Molecules	CHO	CHON	CHOS	CHONS	Total
RS WSOM	Photolysis	Resistant (n)	1731	2624	183	187	4725
		Degraded (n)	200	337	122	170	829
		Produced (n)	393	1165	82	18	1658
		Percentage of degraded in fresh (%)	3.60	6.07	2.20	3.06	14.9
		Percentage of produced in aged (%)	6.16	18.3	1.28	0.38	26.0
	· OH photooxidation	Resistant (n)	919	1030	116	70	2135
		Degraded (n)	1012	1930	189	287	3418
		Produced (n)	904	1813	460	160	3337
		Percentage of degraded in fresh (%)	18.2	34.8	3.40	5.17	61.6
		Percentage of produced in aged (%)	16.5	33.1	8.41	6.97	61.0
YL WSOM	Photolysis	Resistant (n)	1480	1347	717	389	3933
		Degraded (n)	219	408	285	269	1181
		Produced (n)	703	868	215	37	1823
		Percentage of degraded in fresh (%)	4.28	7.98	5.57	5.26	23.1
		Percentage of produced in aged (%)	12.2	15.1	3.74	0.93	31.7
	· OH photooxidation	Resistant (n)	779	702	279	31	1791
		Degraded (n)	920	1053	723	627	3323
		Produced (n)	1010	1097	233	31	2371
		Percentage of degraded in fresh (%)	18.0	20.6	14.1	12.3	65.0
		Percentage of produced in aged (%)	24.3	26.4	5.60	1.70	57.0

Table S5. The information of number and intensity-weighted average elemental ratios, DBE_w, DBE/C_w, $AI_{mod,w}$ and $NOSC_w$ for condensed aromatic compounds produced during ·OH photooxidation in RS and YL WSOM.

Samples	Composition	Number	MW_w	H/C_w	O/C_w	O/N_w	O/S_w	DBE_w	DBE/C_w	$AI_{mod,w}$	$NOSC_w$
	CHO	127	394	0.58	0.21			18.7	0.75	0.75	-0.16
	CHON	380	601	0.61	0.16	2.25		28.4	0.77	0.80	-0.05
RS WSOM	CHOS	111	426	0.60	0.14		3.69	19.7	0.74	0.73	-0.25
	CHONS	41	524	0.64	0.14	4.34	4.34	23.5	0.73	0.72	-0.20
	Total	659	483	0.60	0.16	0.95	1.37	22.6	0.75	0.76	-0.15
	CHO	55	377	0.53	0.18			19.3	0.78	0.78	-0.18
	CHON	199	670	0.55	0.15	2.67		33.4	0.78	0.80	-0.06
YL WSOM	CHOS	64	443	0.57	0.12		3.34	21.3	0.75	0.74	-0.27
	CHONS	25	721	0.58	0.10	4.73	4.73	35.3	0.74	0.74	-0.28
	Total	343	529	0.56	0.14	1.26	1.27	26.2	0.77	0.77	-0.16

Table S6. The intensity-weighted average elemental ratios, DBE_w, DBE/C_w, $AI_{mod,w}$ and $NOSC_w$ for molecular resistant, degraded and produced after photolysis and ·OH photooxidation in RS and YL WSOM.

| Samples	Aging processes		MW_w	H/C_w	O/C_w	O/N_w	O/S_w	DBE_w	DBE/C_w	$AI_{mod,w}$	$NOSC_w$
RS WSOM	Photolysis	Resistant in fresh	249	1.19	0.38	1.02	0.14	6.36	0.51	0.45	-0.35
		Resistant in aged	278	1.17	0.43	1.24	0.09	6.95	0.51	0.42	-0.24
		Degraded	392	1.29	0.33	2.43	2.51	8.83	0.44	0.33	-0.42
		Produced	472	1.07	0.49	4.23	0.28	12.0	0.54	0.43	0.069
	· OH photooxidation	Resistant in fresh	226	1.16	0.41	0.83	0.11	5.93	0.53	0.47	-0.28
		Resistant in aged	278	1.18	0.58	1.27	0.09	6.22	0.51	0.37	0.042
		Degraded	351	1.31	0.27	1.89	0.50	8.24	0.42	0.36	-0.63
		Produced	423	1.10	0.61	3.43	0.71	10.30	0.53	0.35	0.25
YLWSOM	Photolysis	Resistant in fresh	227	1.03	0.46	1.59	1.03	6.49	0.61	0.56	0.067
		Resistant in aged	256	1.02	0.43	0.78	0.60	7.39	0.59	0.53	-0.095
		Degraded	403	1.09	0.38	2.94	2.86	11.18	0.55	0.50	-0.041
		Produced	458	1.03	0.46	2.60	0.67	12.51	0.55	0.44	-0.042
	· OH Photooxidation	Resistant in fresh	208	1.01	0.48	1.53	0.84	6.02	0.63	0.57	0.11
		Resistant in aged	254	1.02	0.55	0.80	0.12	6.82	0.59	0.50	0.12
		Degraded	355	1.10	0.35	2.16	2.37	9.88	0.54	0.47	-0.20
		Produced	425	1.03	0.60	1.84	0.18	10.59	0.55	0.39	0.20
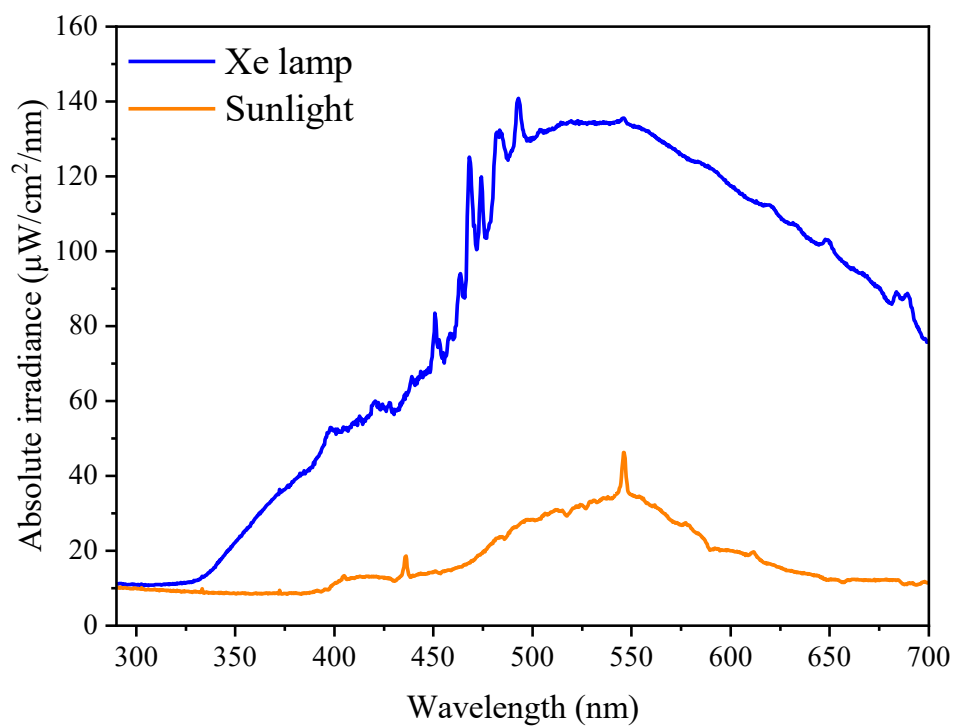
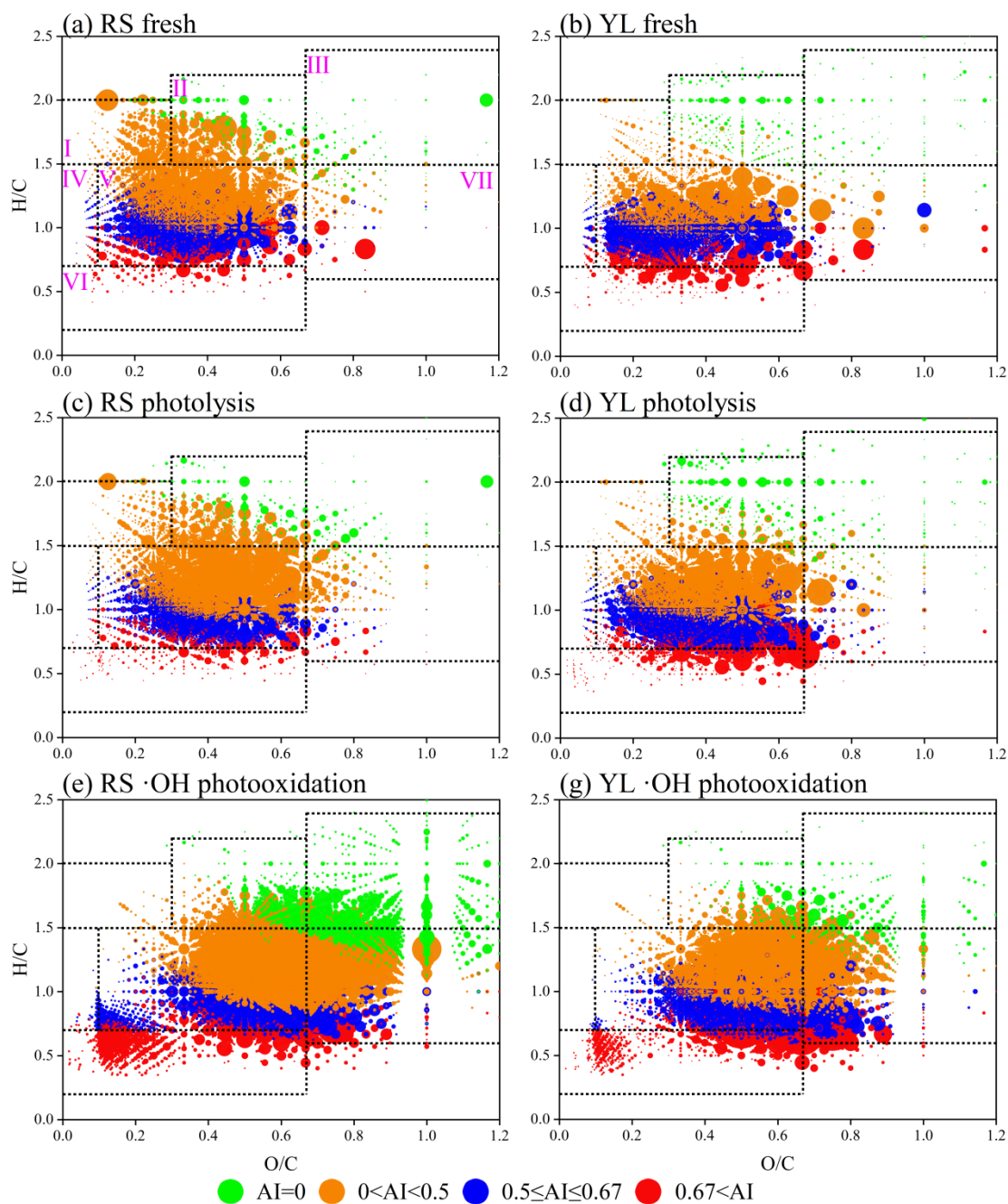**Fig. S1** Spectra of Xe lamp and actual Sunlight (obtained at noon of May 20, 2023, Guangzhou)

Fig. S2 Van Krevelen diagrams of molecular formulas in RS WSOM (a: fresh, c: photolysis, e: ·OH photooxidation) and YL WSOM (b: fresh, d: photolysis, f: ·OH photooxidation). The seven regions represent: I lipids-like, II protein /aliphatic sugar, III carbohydrates, IV unsaturated hydrocarbon, V lignin/CRAM-like, VI condensed aromatic, VII tannins.
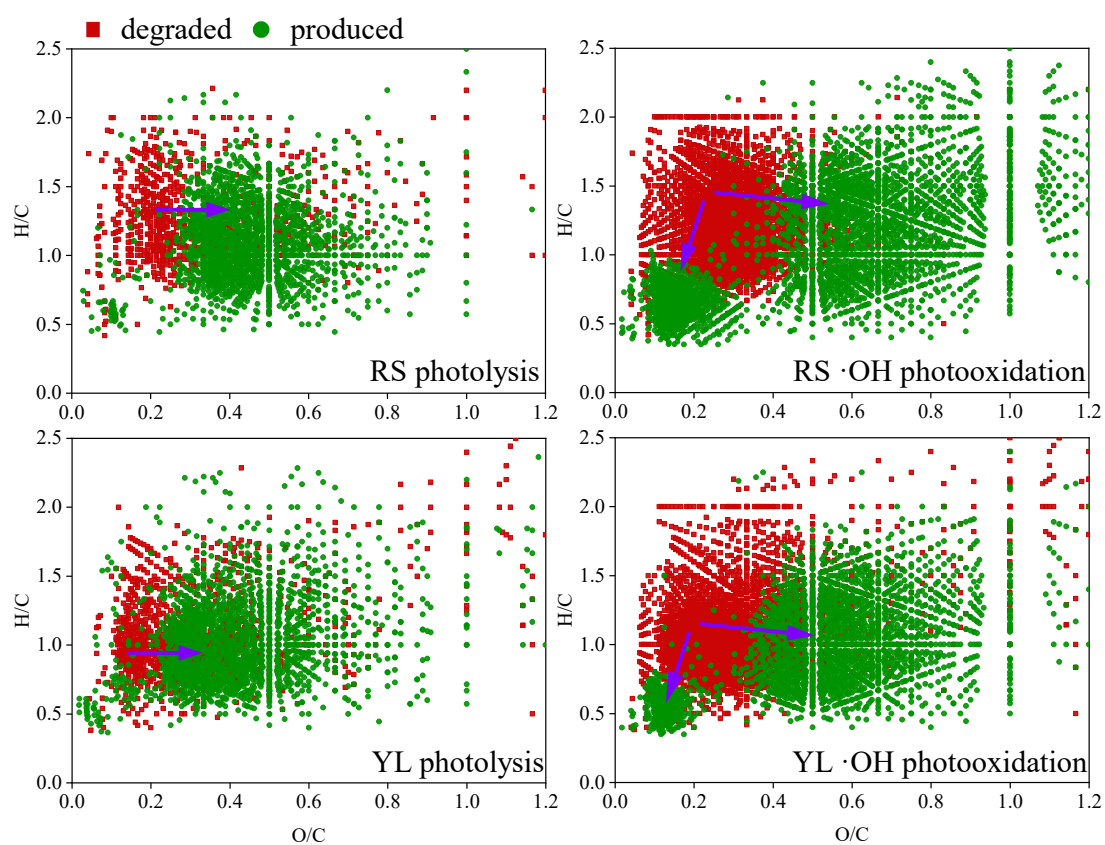
Fig. S3 Van Krevelen diagrams for molecules degraded and produced during photolysis and ·OH photooxidation within RS (upper) and YL WSOM (bottom).

References:

Fan, X., Yu, X., Wang, Y., Xiao, X., Li, F., Xie, Y., Wei, S., Song, J., and Peng, P. A.: The aging behaviors of chromophoric biomass burning brown carbon during dark aqueous hydroxyl radical oxidation processes in laboratory studies, Atmospheric Environment, 205, 9-18, 10.1016/j.atmosenv.2019.02.039, 2019.

Hecobian, A., Zhang, X., Zheng, M., Frank, N., Edgerton, E. S., and Weber, R. J.: Water-Soluble Organic Aerosol material and the light-absorption characteristics of aqueous extracts measured over the Southeastern United States, Atmospheric Chemistry and Physics, 10, 5965-5977, 10.5194/acp-10-5965-2010, 2010.

Jiang, H., Li, J., Sun, R., Tian, C., Tang, J., Jiang, B., Liao, Y., Chen, C.-E., and Zhang, G.: Molecular Dynamics and Light Absorption Properties of Atmospheric Dissolved Organic Matter, Environmental science & technology, 55, 10268-10279, 10.1021/acs.est.1c01770, 2021.

LaRowe, D.E. and Van Cappellen, P.: Degradation of natural organic matter: A thermodynamic analysis. Geochimica et Cosmochimica Acta, 75, 2030-2042, 10.1016/j.gca.2011.01.020, 2011.